Article

Reconstructing Historical Changes in Combustion Patterns by Means of Black Carbon and PAH Evaluation in Dated Sediments from Guanabara Bay, Rio de Janeiro

Cristiane R. Mauad,[a] Angela de L. R. Wagener,*,#,[a] Cássia de O. Farias,[a]
Naira M. S. Ruiz,[b] Renato S. Carreira,[a] Crisógono Vasconcelos,[c] José M. Godoy,[a]
Sonia M. C. de Menezes,[b] Arthur de L. Scofield[a]

[a]LABMAM, Departamento de Química, Pontifícia Universidade Católica do Rio de Janeiro,
20453-900 Rio de Janeiro-RJ, Brazil.

[b]CENPES-PETROBRAS, Avenida Horácio Macedo, 950, Cidade Universitária,
Ilha do Fundão, 21941-915 Rio de Janeiro-RJ, Brazil.

[c]Laboratory of Geomicrobiology, ETH/Zürich, Sonneggstrasse 5, 8092 Zürich, Switzerland.

O histórico de acumulação em sedimentos de produtos de combustão produzidos na área metropolitana ao redor da Baía de Guanabara foi avaliado através de black carbon (BC) e hidrocarbonetos policíclicos aromáticos (HPA) como indicadores. A concentração de BC variou de 0,23-0,51%, com uma tendência crescente de acúmulo de massa ao longo dos últimos 118 anos, mas a proporção BC/carbono orgânico caiu nos últimos 30 anos, possivelmete reflexo de eutrofização. Observaram-se as maiores concentrações de HPAs pirolíticos nos períodos entre 1925 e 1976, condizendo com o período subsequente de desmatamento, urbanização e industrialização que ocorreu na bacia da Guanabara. Estes HPAs foram melhor caracterizados pelo índice diagnóstico BFl/(BFl+BePy). Os dados obtidos permitiram caracterizar os principais eventos que influenciaram o padrão dos produtos de combustão: queima de biomassa e de derivados de petróleo, a crise econômica nos anos 1970 e 1990 e a entrada de etanol na matriz energética brasileira.

The accumulation history of combustion products from the metropolitan area around Guanabara Bay was evaluated using black carbon and polycyclic aromatic hydrocarbons as indicators. BC concentration varied between 0.23 and 0.51%, with an increasing mass accumulation tendency over the last 118 years, whereas a decrease in the values of the ratio BC/organic carbon was observed in the upper sediment layers, probably reflecting the enhancement of bay's eutrophication process in the last 30 years. Higher concentrations of pyrolytic PAH were observed between 1925 and 1976, being consistent with the subsequent deforestation, urbanization, and industrialization that occurred in the Guanabara basin in the period. These PAHs were best characterized by the BFl/(BFl+BePy) diagnostic ratio. The data obtained allowed the characterization of the main events that influenced the combustion patterns in the region: burning of biomass and fossil fuel, economic crisis of 1970 and 1990 and the introduction of ethanol in the Brazilian energetic matrix.

Keywords: black carbon, PAH, geochronology, ^{13}C NMR, SEM/EDX

Introduction

Particles derived from incomplete combustion processes are abundantly present in urban environments[1] and are often responsible for the occurrence of cardiovascular and respiratory diseases in urban population.[2]

Environmental measurements of Black Carbon (BC) are of high importance because it is an exclusively terrestrial contaminant derived from combustion processes. The presence of this combustion residue associated with high molecular weight polycyclic aromatic hydrocarbons (5-6 rings PAH) in sediments of urbanized estuaries derives in great part from the atmospheric deposition of products emitted by mobile sources such as motor vehicles, boats and ships.[3-5] Emissions from industrial sources and from biomass combustion also play a role in

*e-mail: angela@puc-rio.br
#present address: Faculdade de Oceanografia, Universidade do Estado do Rio de Janeiro, 20550-013 Rio de Janeiro-RJ, Brazil

contributing to the pool of recalcitrant organic carbon in sediments.[6,7]

Recent studies[8-10] identify BC as an important sorbent phase for organic hydrophobic contaminants (PAH, dioxins and polychlorinated biphenyls, for instance), principally if the compounds originate from similar sources.[11] Koelmans *et al.*[2] propose that when BC is present in sediments the bioavailability of these contaminants may decrease as much as by two orders of magnitude. The relevance of BC as a sorbent phase was studied by Cornelissen and Gustafsson[12] who suggested that BC may represent 1 to 15% of the total organic carbon (TOC) in sediments of coastal environments.

Coastal environments such as bays, estuaries and lagoons are efficient sinks for natural and anthropogenic material derived from land.[13] The Guanabara Bay in Rio de Janeiro, Brazil, is a highly impacted urban estuary. The system is severely contaminated by inputs from untreated domestic and industrial effluents and may serve as the final destination for atmospheric contaminants derived from the dense vehicular traffic in the several municipalities circumscribing the bay, and from other activities.

A single report on the presence of BC in surface sediments of the Guanabara Bay is provided by Ribeiro *et al.*[10] which found concentrations varying between 0.03 and 0.31%.

The aim of the present work was to investigate for the first time the historical development of combustion processes in the hydrographic basin of the Guanabara as recorded in a sediment core using BC associated with high molecular weight (HMW) PAH (benzo(b)fluoranthene, benzo(k,j)fluoranthene, benzo(a)pyrene, benzo(e)pyrene, Indeno(1,2,3-cd)pyrene, dibenz(a,h)anthracene and benzo(g,h,i)perylene) as markers of incomplete combustion to observe the transition (qualitatively and quantitatively) from a predominantly agricultural region in the past and which currently consists of a metropolis with high density of industries and highways. The focus on HMW PAH is justified due to the predominance of these compounds in combustion residues in relation to lower molecular weight PAH and to their persistence in minor degradation rates in sediments.[14]

Study Area

The Guanabara Bay (22°40'-23°00' S and 43°00'-43°20' W) in Rio de Janeiro, Brazil, has a surface area of 384 km² and an average water depth of about 6 m. The 4000 km² hydrographic basin is densely populated housing about 10×10⁶ inhabitants. Uncontrolled urban expansion and development in the Guanabara basin are the root causes of a severe state of deterioration. The major potential pollution sources include intense vehicular traffic, urban drainage, release of untreated domestic sewage and industrial residues, littering and navigation. The bay is circumscribed by major highways (one of them, the Brazil Avenue has an estimated flow of 250,000 vehicles day⁻¹ accounting for 25-30% of the total atmospheric emissions in the metropolitan area of the Rio de Janeiro municipality;[14-16] and crisscrossed by a 14 km long bridge with an estimated traffic of 150,000 vehicles day⁻¹. The second major Brazilian industrial park in the northwestern region of the bay comprises more than 6,000 industries.[17-19] The bay gives support to the exploration, transportation and transformation activities of the expanding petroleum industry

Experimental

Sampling

A sediment core was sampled using a piston corer and a 6 m long aluminum tubing with 7.5 cm i.d.. The sampling station (A) in the northwest area of Guanabara Bay (Figure 1) was selected for the study because it is located in the most contaminated area in the bay.[20] Prior to sampling, side-scan sonar was used to verify the possible presence of pipes or the prior occurrence of dredging so as to avoid sampling in areas where sediments had been disturbed. The sampled core was sectioned in 2 cm layers and in the present work only the upper 72 cm was inspected. The segments were separated into two groups of sub-samples, one used
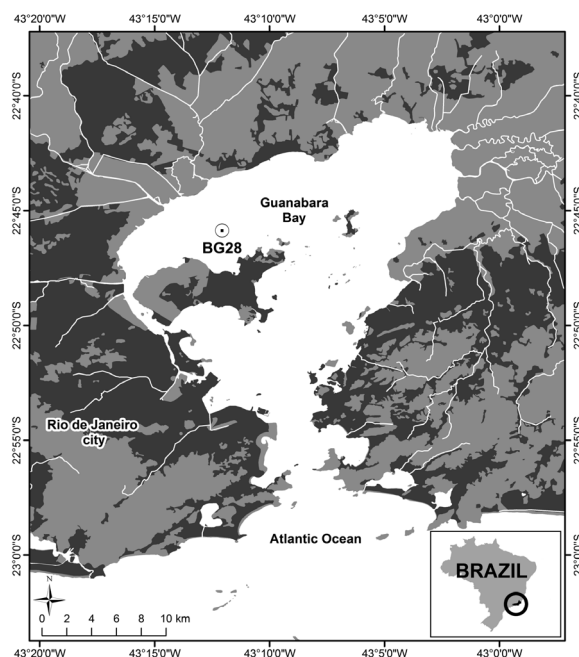
Figure 1. Map of Guanabara Bay showing the sampling station A.

for dating by ^{210}Pb as already reported in Godoy *et al.*,[16] and the other for BC and PAH analysis after storage at –20 °C in decontaminated glass flasks with Teflon caps.

Reagents and chemicals

Hydrochloric acid fuming 37% P.A. (Merck, Darmstadt, Germany), nitric acid P.A (Vetec, Rio de Janeiro, Brazil), hydrofluoric acid 40% P. A. (Vetec), sodium hypochlorite commercial solution (Globo, Rio de Janeiro, Brazil), ultrapure water from Milli-Q, dichloromethane (Mallinckrodt Chemicals, Phillipsburg, NJ, USA), acetone (Mallinckrodt Chemicals), *n*-hexane (Mallinckrodt Chemicals), aromatic surrogate standard p-terphenil-d[14] (AccuStandard, New Haven, USA), solution composed of the standards naphthalene-d[8], acenaphthene-d[10], phenanthrene-d[10], chrysene-d[12], and perylene-d[14] (AccuStandard), standards of 1 and 2-methylnaphthalene, 1,5 and 1,7 dimethyl-phenanthrene and 2,6 and 3,5 dimethyl-phenanthrene (CHIRON AS, Trondheim, Norway). Zinc PA grade (Merck), copper sulfate (Merck), chromium oxide (Alpha, Stevensville, MI, USA) and copper wires (Alpha). Silica gel 60 (0.063-0.200 mm, Merck) was decontaminated for 24 h with dichloromethane in a Soxhlet extractor; when dry, was activated at 170 °C for 12 h and then 5% (m/v) deactivated. Anhydrous sodium sulfate (Merck) and aluminum oxide 90 active neutral (Merck) were muffled at 450 °C for 6 h and after this, the aluminum oxide was 2% (m/v) deactivated.

Analysis

Determination of total organic carbon (TOC), total nitrogen (TN) and black carbon (BC)

For TOC and TN determination, about 10 mg of sample were weighed into silver capsules (Alpha). Carbonates were eliminated by treating samples with 6 mol L^{-1} HCl. The quantification was performed in a Carlo Erba EA1110 elemental analyzer and was based on calibration curves (r > 0.999) using acetanilide as a standard. Quality assurance included the use of reference material sediment NIST 1944 (New York/New Jersey Waterway Sediment) for which the average TOC concentration found (n = 4) of 4.63% ± 0.07% d.w. was within the expected range (4.4 ± 0.3% d.w.). The limit of quantification was of 0.09% d.w. for carbon and of 0.03% for nitrogen.

The methodology for BC quantification - CTO-375 - was initially proposed by Gustafsson *et al.*[8] Freeze dried samples were ground and < 63 μm sieved before carbonate elimination with 6 mol L^{-1} HCl and thermal oxidation under air flow. The temperature program used for oxidation was

as follows: 10 °C min^{-1} to 300 °C, 1 °C min^{-1} up to 375 °C, hold at 375 °C ± 5 °C for 24 hours and after this, decrease (1 °C min^{-1} to 300 °C and 10 °C min^{-1}) to room temperature, in this case, about 30 °C. After the oxidation process only the more refractory carbon fraction remains.

BC determination was carried out in an elemental analyzer using the same procedures as described for TOC. The accuracy of the methodology was checked using the reference material NIST 1941b (Organics in Marine Sediment),[21-23] which has been widely used for this purpose. For each batch of samples (10 samples in triplicate), the analytical control was performed by the simultaneous analysis of reference material (3-4 aliquots). The result for BC found for the reference material in this study was 0.59% ± 0.15 d.w. for n = 19, which, according to Student›s test is statistically similar, at the confidence level of 95%, to that found in collaborative analytical studies (0.53 ± 0.14% d.w., n = 5).

Characterization of BC by scanning electron microscopy (SEM) and energy dispersive X-ray spectroscopy (EDX)

The analysis of scanning electron microscopy was performed in nine samples chosen to represent older, intermediate and recent periods of the observed time span. Although the main goal of this analysis was to visually identify BC forms, samples were inspected without any pre-treatment so as to observe possible aggregation between amorphous organic matter and BC and to evaluate the general composition of the sediment. The scanning electron microscopy was performed in a Zeiss 50 VP microscope coupled to an energy dispersive x-ray spectrometer (EDX). A 6 nm platinum coating was applied. The images and EDX analysis were obtained with a backscatter detector, with accelerating voltage of 12 kV and a working distance of 10 mm.

Characterization of BC by ^{13}C NMR CP/MAS and ^{13}C NMR CP/MAS-NQS

Approximately 2.0 g of each of the eight analyzed samples were weighed directly into 50 mL Teflon centrifuge tubes, to which 30 mL of 1 mol L^{-1} HCl were added. The samples were shaken for 1 h at room temperature (approximately 30 °C) to remove carbonates and sesquioxides.[24] Then the supernatants were discarded and the remaining mineral fractions were treated with a 1 mol L^{-1} HCl + 10% HF solution, and were agitated for 12 h at room temperature to remove the paramagnetics. The supernatants were removed after centrifugation (15 min at 3500 rpm) and the treatment was repeated once more.

At the end of treatment, the samples were freeze dried for subsequent chemical oxidation treatment of the lignin

fraction and other organic compounds present in the sample which could interfere with the analysis leading to overestimating BC, as suggested by De La Rosa[25] and Simpson and Hatcher.[26] In this step, the freezer dried samples, previously demineralized, were chemically oxidized with a solution of sodium hypochlorite and acetic acid (109 mL of 2% NaOCl, 200 mL of H_2O and 5 mL of CH_3COOH).[26] The samples were agitated for two hours, and then centrifuged at 5000 rpm for 25 min. The process was repeated twice and the residue was then freeze dried.

The NMR analysis was performed in an Infinity Plus spectrometer equipped with probe-400 CP/MAS suitable for analysis of solid samples. The first employed technique was of cross polarization with magic angle spinning (CP/MAS) which, although not a quantitative technique, can be used for comparative analysis when the analyzed materials are similar. The second pulse sequence used was the non-quaternary suppression (NQS), that shows only quaternary and methyl carbons in the sample. Both analyses were made under almost the same experimental conditions, except for the non-quaternary suppression that uses the decoupled time of 50 µs. The other experimental conditions valid for both ^{13}C NMR analysis were: frequency of 100.26 MHz, spectral width of 50 kHz, acquisition time of 20.48 ms, pulse of 90° (2.75 µs), pulse delay of 1.0 s, contact time of 1000 µs, 50000 transients, rotor of 4.0 mm, spinning speed of 10000 Hz; the peaks were referred to HMB (hexamethylbenzene - methyl peaks at 17.3 ppm) and processed with an line broadening (lb) of 300 Hz.

PAH determinations

The methodology used for PAH extraction was based on EPA 3540C method. To approximately 1 g of dried and homogenized sediment 100 ng of *p*-terphenyl-d$_{14}$ was added as surrogate standard to monitor the effectiveness of the analytical process. After 24 h of Soxhlet extraction in a 1:1 mixture of dichloromethane-acetone (Suprasolv, Merck), extract volume was reduced in a rotary evaporator prior to solvent exchange to hexane.

Clean up proceeded in a glass column (1.3 i.d. and 30 cm height) packed in the top with colloidal copper for sulfur removal, followed by 2 g of anhydrous Na_2SO_4, alumina (1 g, 2% water deactivated) and silica gel (11 g, 230-400 mesh, activated at 160 °C). The aliphatic fraction was eluted with 50 mL hexane followed by PAH elution with 50 mL of a 1:1 hexane-dichloromethane mixture followed by rotary evaporation of the extracts.

The extracts were quantitatively transferred to 1 mL volumetric flasks and volumes were completed with hexane. PAH determinations were performed in a GC/MS (Finnigan Trace gas chromatograph coupled to a Finnigan

Polaris Q mass spectrometer) system fitted with a J&W XL-ITD capillary column (30 m × 0.25 mm × 0.25 µm), operating in SIM mode. Helium was used as carrier gas adjusted at 1.2 mL min^{-1} and the column temperature was programmed as follows: initial hold of 5 min at 50 °C, 50 °C min^{-1} up to 80 °C, 6 °C min^{-1} from 80 °C to 280 °C and a hold of 25 min at 280 °C. The injector temperature was at 270 °C (interface at 300 °C and ion source at 250 °C; electron impact 70 eV and emission current 250 µA) and the injected volume was 2 µL. Quantification included the following PAH compounds: benzo(a)pyrene (BaPy), benzo(e)pyrene (BePy), benz(a)anthracene (BaA), benzo(b)fluoranthene (BbFl), benzo(k,j)fluoranthene (BkFl), indeno(1,2,3-*cd*)pyrene (IP), dibenz(a,h)anthracene (DBahA), benzo(*ghi*)perylene (BghiPe), perylene (Pe), 1,7-dimethylphenanthrene and 2,6-dimethylphenanthrene. Internal standards used for quantification contained a mixture of crysene-d$_{12}$ and pyrene-d$_{12}$. Quantification of the alkylated PAH was based on the calibration curve of the 1,7- and 2,6-dimethylphenanthrenes for which standards were available.

The analytical control of the process included checking the concentration of PAH contained in standards solutions prepared with different analyte concentrations (5, 10, 20, 50, 100, 200, 400 and 1000 ng mL^{-1}). Linear correlation coefficients > 0.990 were obtained for the calibration curves in all cases. In addition, for each group of 10 analyzed samples a standard solution of the above compounds was injected to check instrumental calibration conditions. The detection limit ranged of 0.14 to 0.64 ng g^{-1} and the quantification limit obtained was < 2.00 ng g^{-1}. The accuracy was tested through successful analysis of SRM-NIST 1944.

Statistical Evaluation

Statistical evaluation included Spearman correlation test and Mann-Whitney U test using the software Statistica 9.0.

Results and Discussion

The entire data set is shown in Tables 1-3.

TOC and TN geochronology

The average concentration is of 3.5 ± 0.58% with a maximum of 4.6% in the upper layer and a minimum of 2.5 % at 43 cm depth. The organic carbon content in the upper layer was within the range of 4.02% < TOC < 5.28% reported by Ribeiro *et al.*[10] for surface sediments in the bay.

In the time interval of 118 years registered in the core, TOC shows an increasing trend from past to present (r = 0.773; p << 0.05; slope = 0.012% year^{-1}). The analysis

of the data for the period after 1960 shows that the increasing TOC concentration trend is more pronounced (r = 0.764; p << 0.05; slope = 0.032% year^{-1}). This may principally derive from: (1) the increasing input of organic material due to sewage discharge and fertilization of the system following the large population growth. While in the period of 80 years, from 1890 to 1960, the population in the region of Rio de Janeiro increased from 5.2×10^5 to 3.2×10^6 inhabitants,[27] in the subsequent 45 years the population almost triples, reaching 10×10^6 inhabitants. The population density within the limits of the Guanabara watershed increased even more notably in the latter period (population estimates are of 8×10^6 inhabitants). The absence of effective sewage treatment systems led to (1) a profound eutrophication of the bay; (2) increase over time of overall sedimentation of solids; and (3) natural decay of organic matter. The depth profiles for TOC concentration and for TOC-mass accumulation rate (TOC MAR) are given in Figure 2 and show that, in general, TOC co-varies with TOC MAR up to 1990 and thereafter increases while the MAR decreases. The co-variation of TOC and TOC MAR reveals that prior to 1990 TOC depends principally on the sedimentation rate while in the last two decades TOC increases despite the decreasing trend in sedimentation rates. As the average variation in TOC concentration is of only 16%, degradation in the typically anoxic sediments seems to be limited. Wagener[28] observed that organic matter oxidation by nitrate and sulfate reduction is restricted to the upper 7 cm of these sediments. Therefore, the increasing trend in TOC concentration in the last 20 years can be ascribed, in great part, to a net increase in apportioning of organic carbon to the sediments. Similar trends are also found for total nitrogen. Since the regression line that correlates TOC and TN (r = 0.91; n = 30, p = 0.0000) crosses the TOC axis at a positive value in TN = 0, the presence of ammonium may be considered not significant; in such case TN is approximately equal to the organic nitrogen content.

The average molar C/N ratio (see Table 1) of 10.97 ± 0.96 indicates mixture of marine and land-derived organic matter. For instance, simple mass balance considering two end-members with C/N values of 7 and 0, respectively, for autochthonous and allochthonous material,[29] revealed a range between 30-40% for the fraction of terrestrially-derived material in the sediment. In addition, some of the observed C/N maxima (e.g., 12.5, 12.7 and 13.5) coincide with historical records of massive rain fall,[27] which resulted in extraordinary soil erosion and increased inputs from land.

BC geochronology

BC determined by the combustion method comprises mainly soot particles and may principally stand for emissions from liquid fossil fuel combustion in mobile and stationary sources. Although the automotive fleet grew exponentially since mid-1960s as reported by the Brazilian Automotive Industry Association,[30] BC showed no statistically significant (p < 0.05) changes in average concentration found between the time period prior to 1958 ($0.34\% \pm 0.095\%$) and for the period 1960-2005 ($0.37\% \pm 0.071\%$). According to the cited source, the number of newly licensed vehicles in 1970 in Brazil was of 2×10^6 increasing to more than 50×10^6 by 2005. The increasing rate for the country is reflected in the greater Rio de Janeiro area (includes the city of Rio and other 14 municipalities). Presently, in the city of Rio de Janeiro there are about 2×10^6 licensed vehicles. The lack of an anticipated increase in BC accumulation in the sediments may be due to a combination of factors: wider atmospheric dispersion of soot particles (< 1 μm) produced by fuel combustion, which may settle distant from the emission area;[5,31] efficiency of tidal currents in the Guanabara Bay[32] which can drive these particles to the outer areas before they undergo aggregation and transport to sediments in the bay, and the increasing ethanol use since 1979 as fuel in mixtures of up to 25% in gasoline. It has been reported[33] that the mixture of ethanol-gasoline in the ratio 20/80 reduces by up to 50% de emissions of soot.

Although the factors cited above might have influenced the sedimentary BC record, the trends in BC appear divisible into three periods where a slight increasing trend ($r \geq 0.637$; p < 0.05) is registered: 1880-1955 with an increasing rate of 0.003% year^{-1}, 1958-1978 with an increasing rate of 0.01% year^{-1} and 1979-2005 with a rate of 0.006% year^{-1}. The largest increase rate in BC corresponds to the period
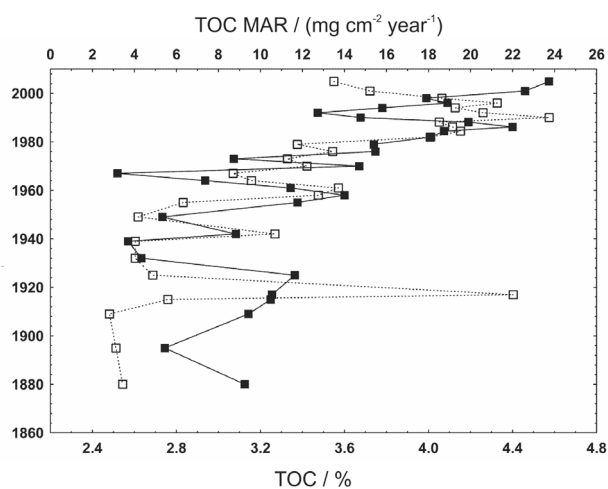
Figure 2. Depth profile of TOC concentration (closed squares) and TOC Mass Accumulation Rate (TOC MAR; open squares).

(1956-1978) when industrialization of Rio de Janeiro grew exponentially in the northwestern region of the Guanabara basin, including commissioning of the second largest refinery in Brazil and peaks in gasoline and diesel fleets. The lowest rate in the period 1979-2005 may be ascribed to the decrease in emissions due to the use of ethanol and more recently the modernization of the motor vehicles as will be discussed in further details under item PAH geochronology.

In contrast to BC, the BC MAR data (Figure 3), shows lesser scattering and a statistically significant increasing trend of 0.012 mg cm^{-2} year^{-2} (r = 0,577; p << 0.05) can be observed along the 118 year period covered by the core. This is equivalent to about 70% increment, on the average, increment in the BC mass accumulation rate during the period.
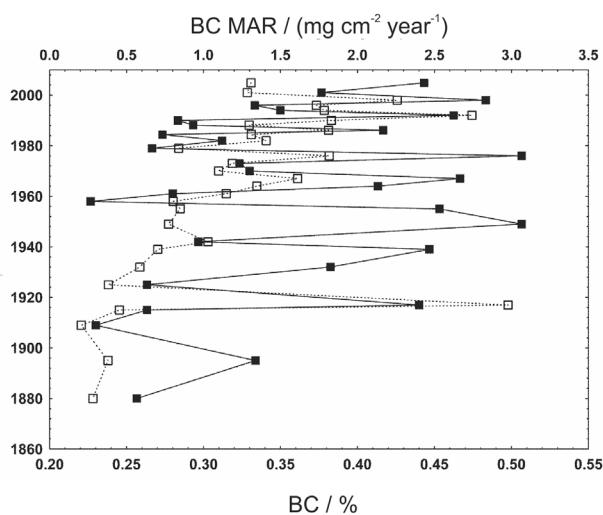
Figure 3. BC concentration (closed squares) and BC Mass Accumulation Rate (BC MAR; open squares).

There is lack of significant correlation between BC and TOC concentrations. This is expected since TOC is principally comprised of amorphous organic carbon deriving from processes unrelated to combustion. Such feature has been observed in other coastal sediments.[7] The fraction of BC to TOC ranged from 6.3% to 18.5% (Table 1). Despite the large scatter in the data set, a trend of increasing values was observed up to the late 1960s, indicating a higher accumulation of BC in Guanabara Bay sediments over this period. For more recently deposited sediments, however, an opposite trend was observed, i.e., the contribution of BC to the pool of organic carbon decreased. This suggests that the significant increase in the autochthonous carbon storage in sediments of Guanabara Bay, observed in the last decades following sewage addition and eutrophication,[20] was more significant than any increase in BC associated with urban development and fuel combustion.

The levels of BC/TOC reported here are similar to those given in Luz *et al.*[34] (2.3% to 12.8% in surface sediments of Guanabara Bay), in Accardi-Dey and Gschwend[35] (6- 22% in the Boston Harbor) and in Rockne *et al.*[36] (12-13% in sediments from New York and New Jersey Harbors).

BC determinations by SEM/EDX and NMR

In the present work 9 segments of the core (segments: 3, 15, 33, 39, 45, 51, 55, 59 and 71) were selected for the SEM/EDX analysis. The EDX improves significantly the results from the SEM in studies of BC, by showing qualitative aspects of the chemical composition of the examined particles.[37] A limitation is that this technique allows analysis only of a small fraction of the particles under observation.[38]

All observed segments showed the presence of large quantities of amorphous organic matter derived from intense microbiological activity. Remains of centric diatoms were very abundant (see Figure S1 in Supplementary Information) as expected, since these algae are profusely present in nutrient rich environments. Some crystalline structures were also observed in the sample. Only in the segment 15 (deposited around 1992) BC was unequivocally detected as can be verified in Figure 4. The size and morphology of the particles coincide with those described for BC by Glaser *et al.*,[39] Song *et al.*[40] and Brodowski *et al.*.[38] The elevated content of carbon and oxygen as well as the incidence of chlorine and sulfur detected by EDX confirms the presence of BC particles. Such composition has been ascribed to BC particles possibly (see Figure 4 and 5) originated from biomass combustion.[41] In the present case, the spherical structure, however, suggests BC originated from fossil fuel combustion. This uncertainty as to the origin may be an artifact derived from aging and processing of soot particles in the atmosphere, which can change the original composition thereby decreasing the initial carbon content and incorporating other elements.[42] The analysis also shows in this sample the presence of calcium carbonates and aluminum oxides (Figure 5).

The sedimentation of BC particles of about 1 µm in size must involve aggregation with other materials present in the water column, however the observed BC particles appear isolated in the SEM even though this may result from degradation of the labile components of the original aggregates once in the sedimentary environment. The detection of BC particles in other segments was not effective due to interferences of major components of the matrix, since samples were examined without prior treatments to eliminate carbonates, oxides and amorphous organic material.

Table 1. Total organic carbon (TOC), black carbon (BC), total nitrogen (TN) concentrations, C/N ratio, sedimentation rates and mass accumulation rates

Segment / cm	Year	TOC / %	BC / %	OC / %	BC/TOC/ %	TN / %	C/N / (mol L⁻¹)	SAR / (g cm⁻² year⁻¹)ᵃ	TOC MAR / (mg cm⁻² year⁻¹)	BC MAR / (mg cm⁻² year⁻¹)
1	2006							0.60		
3	2005	4.57	0.44	4.13	9.69	0.58	9.20	0.30	13.50	1.31
5	2001	4.46	0.38	4.08	8.45	0.49	10.62	0.34	15.21	1.28
7	1998	3.99	0.48	3.51	12.11	0.52	9.01	0.47	18.64	2.26
9	1996	4.09	0.33	3.76	8.15	0.41	11.64	0.52	21.27	1.73
13	1994	3.78	0.35	3.43	9.26	0.37	11.92	0.51	19.27	1.78
15	1992	3.47	0.46	3.01	13.32	0.39	10.32	0.59	20.60	2.74
17	1990	3.68	0.28	3.39	7.71	0.41	10.55	0.65	23.75	1.83
27	1988	4.19	0.29	3.90	7.00	0.46	10.55	0.44	18.52	1.30
29	1986	4.40	0.42	3.98	9.47	0.48	10.69	0.44	19.14	1.81
31	1984	4.07	0.27	3.80	6.71	0.44	10.80	0.48	19.52	1.31
33	1982	4.01	0.31	3.70	7.78	0.41	11.42	0.45	18.08	1.41
35	1979	3.74	0.27	3.47	7.13	0.42	10.47	0.31	11.76	0.84
37	1976	3.75	0.51	3.24	13.52	0.44	10.01	0.36	13.44	1.82
39	1973	3.07	0.32	2.75	10.52	0.33	10.98	0.37	11.28	1.19
41	1970	3.67	0.33	3.34	8.99	0.36	11.89	0.33	12.21	1.10
43	1967	2.52	0.47	2.05	18.52	0.28	10.63	0.35	8.70	1.61
45	1964	2.94	0.41	2.52	14.07	0.28	12.46	0.33	9.57	1.35
47	1961	3.34	0.28	3.06	8.37	0.37	10.45	0.41	13.71	1.15
49	1958	3.60	0.23	3.37	6.30	0.33	12.73	0.35	12.75	0.80
51	1955	3.38	0.45	2.92	13.43	0.42	9.45	0.19	6.32	0.85
53	1949	2.73	0.51	2.23	18.54	0.31	10.29	0.15	4.17	0.77
55	1942	3.08	0.30	2.79	9.62	0.32	11.24	0.35	10.69	1.03
57	1939	2.57	0.45	2.12	17.38	0.27	10.97	0.16	4.04	0.70
59	1932	2.63	0.38	2.25	14.53	0.28	10.97	0.15	4.04	0.59
61	1925	3.36	0.26	3.10	7.83	0.36	11.00	0.15	4.88	0.38
63	1917	3.26	0.44	2.82	13.52	0.29	13.25	0.68	22.03	2.98
65	1915	3.25	0.26	2.99	8.11	0.34	11.07	0.17	5.59	0.45
67	1909	3.14	0.23	2.91	7.32	0.34	10.89	0.09	2.82	0.21
69	1895	2.75	0.33	2.41	12.16	0.27	11.89	0.11	3.13	0.38
71	1880	3.13	0.26	2.87	8.21	0.31	11.67	0.11	3.44	0.28

ᵃGodoy *et al.*;[16] MAR: Mass Accumulation Rate; SAR: Sediment Accumulation Rate.

The CP/MAS ^{13}C NMR analysis has been successfully used as a non-destructive technique in studies of organic matter in soils and sediments.[43] The pretreatments so far applied to remove silica oxides, paramagnetic elements and lignin were necessary to obtain a reliable response in the NMR analysis.[24,26,44]

The ^{13}C NMR spectrum is divided into the following regions: 0-50 ppm corresponding to alkylated carbons; 50-100 ppm to oxygenated aliphatic carbons; 110-160 ppm to aromatic carbon; 150-190 ppm to phenols and carboxyl; and 190-220 ppm to carbonyl groups.[26,45,46]

In all samples, before chemical oxidation, a significant content of aliphatics and polysaccharide rings (in the region of 73 ppm) were observed. According to Lu *et al.*[45] these polysaccharide rings are related to the presence of cellulose although the occurrence of fibrous structure was not clear from the SEM of the examined sediments. In the present case, algae and bacteria polysaccharides are the most probable source of the signal in the region of 73 ppm.

After oxidation with hypochlorite and acetic acid, the entire aromatic component in the region between 110 and 140 ppm can be considered as BC in the forms of charcoal,
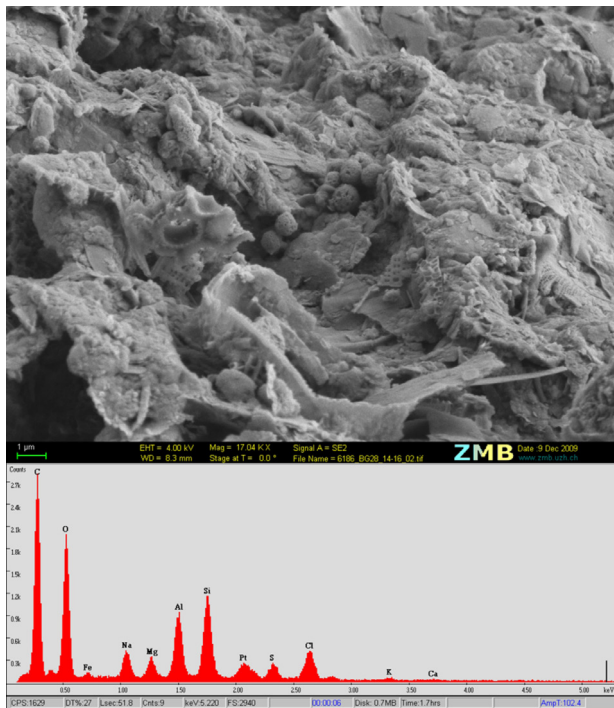
Figure 4. SEM/EDX of segment 15 showing spherical particles of BC and the elemental composition of the particles.

soot and other reduced carbon.[26] In Figure 6 a decrease in signal in the aromatic region can be observed in different intensities for several segments after chemical oxidation, confirming the need for this treatment to avoid overestimating BC in NMR analysis. BC contents obtained by using different analytical techniques cannot be compared, still the NMR determination proved the presence of recalcitrant aromatic carbon in all but two of the tested samples. The relative content of quaternary and unsubstituted carbons in the region of aromatic compounds of the NMR spectrum was determined by ^{13}C CP/MAS-NQS after chemical oxidation. Table 2 shows the results for these fractions of the aromatic carbon for each analyzed sediment segment. For the segments 59 and 71 it was not possible to obtain the relative content because of the extremely low carbon content after chemical oxidation. In segment 3 both the refractory and the less condensate BC species were present in equal proportions. In the other samples unsubstituted carbons predominated over the quaternary carbons suggesting biomass combustion as a major BC source.

It is possible to infer from the development of the anthropogenic activities in the Guanabara basin that
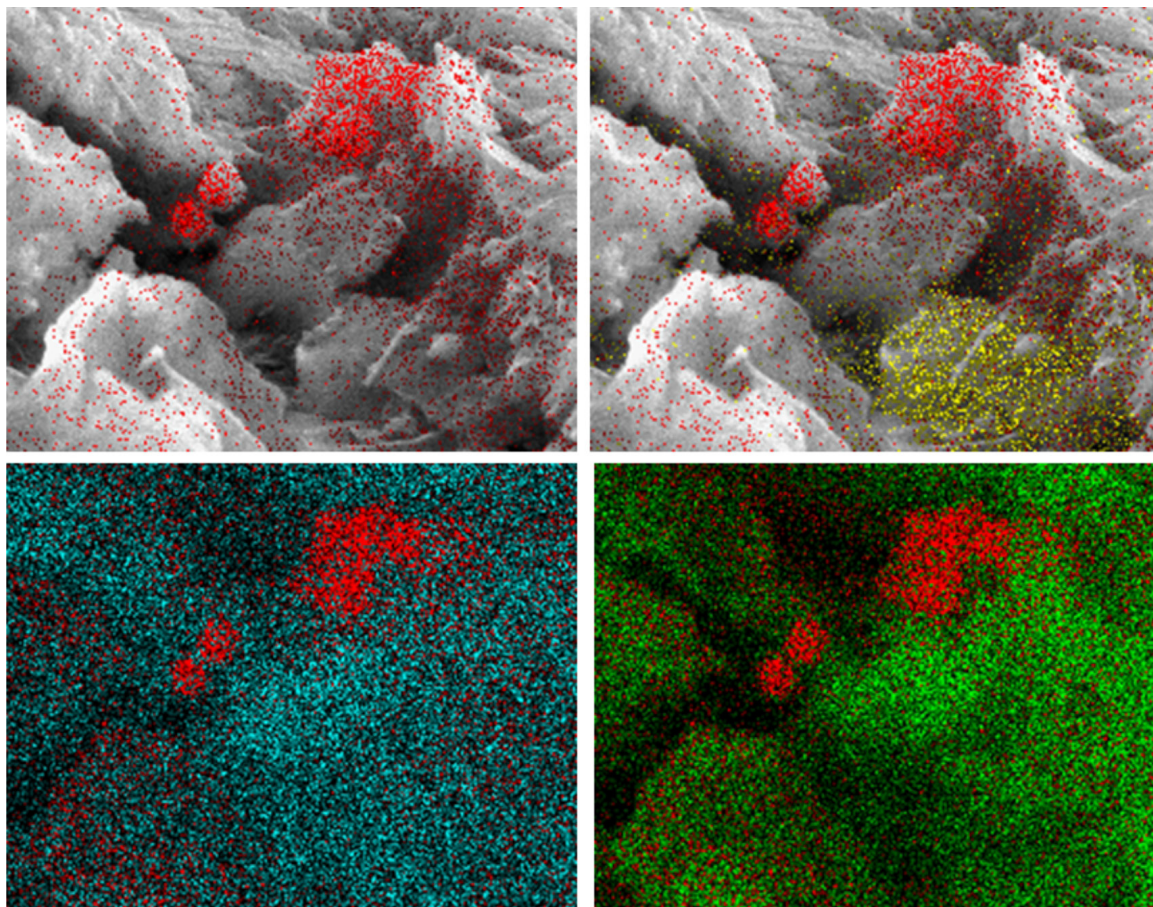
Figure 5. SEM/EDX of segment 15 showing the areas enriched in carbon (red), calcium (yellow), oxygen (blue) and aluminum (green).

Table 2. Determination of aliphatic and aromatic content (%) by NMR in segments of core BG 28

Segment	Aromatic BO / % (110-200 ppm)	Aromatic BO / % (110-140 ppm)	Aromatic AO / % (110-140 ppm)	Quartenary AO / %	Unsubstituted aromatic AO / %	Aliphatic / %
3	23.8	12.0	9.5	5.0	4.5	76.2
33	22.3	14.0	12.0	3.0	9.0	77.7
39	30.2	11.6	8.0	1.0	7.0	69.8
45	30.6	15.6	15.6	1.3	14.3	69.4
55	25.9	13.6	13.0	4.7	8.9	74.1
59	18.6	9.5	9.5	ND	ND	81.4
65	24.5	11.6	12.0	4.8	7.2	75.5
71	19.8	10.6	ND	ND	ND	0.82

ND: Not detected; BO: before oxidation; AO: after oxidation.
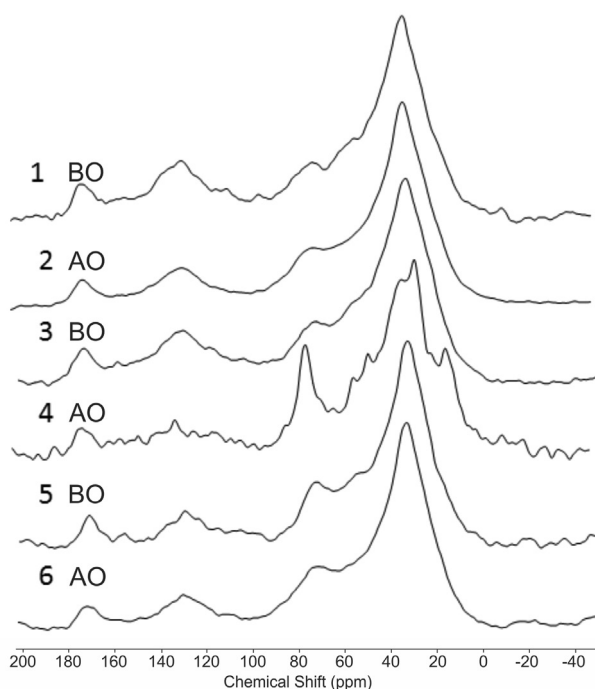
Figure 6. Examples of NMR spectra before oxidation (BO) and after oxidation (AO), respectively: segments 3 (1 and 2), 39 (3 and 4) and 59 (5 and 6).

samples from 1880 to mid-1950s should contain material principally derived from biomass combustion. Agricultural activities in Brazil were historically based on the preparation of the land using the slash-and-burning approach or by clearing the fields by burning grass and shrubs. However, the combustion matrix changed over the examined period; biomass combustion decreased from the past to present time followed by an intense increase in fossil fuel combustion, especially after the 1970s. As discussed under item BC Geochronology, the efficient atmospheric transport of soot particles formed in liquid fossil fuel combustion, may be one factor explaining the discrepancy between BC sedimentary records and historical developments.

PAH geochronology

Table 3 displays the results for the HMW PAH. In Figure 7 the sum of the 5-6 rings PAH shows an increasing trend from 1880 to 1960s followed by a decrease with time to the present. The PAH MAR display similar general features. In recent years the most notable increase in PAH is observed around 2001. This increase may be associated with a MF380 oil spill that affected the northwestern area of the bay in 2000. This oil is enriched in heavy PAH[14] and may have contributed to the higher concentrations in segment 5.

The increasing trend in pyrolytic PAH between 1880 and the 1960s is coherent with the subsequent deforestation, urbanization, and industrialization that occurred in the Guanabara basin in the period. However, similar to the observed BC trends, the more pronounced developments after the 1960s are not apparent in the sediments. For instance, the impacts derived from the intensification of vehicular and ship traffic in the Guanabara basin during the period between 1980-2006 due to fast population growth are not evident.

The variations in sediment accumulation rates (SAR) seem to influence PAH record in different ways, for instance, the decrease by a factor of 2.5 in the SAR (see Table 1) from 1990 to 2006 is first accompanied by an increase in PAH concentration from 1990 to 1996 and thereafter, except 2001 (just after the oil spill), PAH concentrations tend to vary with the SAR decreasing to values below those found circa 1880. This later trend suggests that a significant fraction of these PAH found their way into the bay through runoff as will be discussed further later. In certain periods (i.e., from 1990 to 1996) an increase in SAR leads to a decrease in concentration indicating, for instance, an attenuation of the PAH inputs. In the period 1915-1939 (except 1917), SAR was rather constant although a steady increase is observed in PAH

concentration due to increasing apportioning from runoff or atmospheric deposition.

A substantive increase in PAH is registered in the period from 1920s to the early 1960s (Table 3; Figure 7). Such result could lead to the assumption that combustion processes in the Guanabara basin were more important in the cited period, decreasing in recent times. However, this indication may in part derive from the combined effect of the decrease in biomass combustion occurring parallel to the growth in fossil fuel combustion from past to present. Submicron soot particles preferably emitted during fossil fuel combustion and loaded with PAH tend to disperse over larger distances, therefore resulting in

reduced atmospheric PAH flux to sediments in areas near the emission sources. To test this hypothesis the ratio of BaPy/BePy was used as indicator of the proximity of combustion sources[47] to the final destination of settling particles, since BaPy undergoes fast photo degradation compared to BePy and both compounds are rather stable once in the anoxic sediment environment. In all examined samples this ratio was very close to unity (1.19 ± 0.18; Table 3), therefore there is no indication through this tool, using the entire data set, of a change in source distance for the settled material. However, if results for the period of 1880 to 1984 are compared with those for 1988 to 2005 (the period of fastest growth in vehicular production)[30]

Table 3. Concentration of pyrolytic PAH ($\mu g\ kg^{-1}$) and diagnostic ratios

Segment	BbFl	BkFl	BePy	BaPy	Pe	IPy	DBahA	BghiPe	2,6DMPh	1,7DMPh	ΣPAH (5-6 rings)	Pe/Σpenta	IPy/ (IPy+BghiPe)	BaPy/ BePy
1	88.16	22.66	59.40	49.92	18.89	36.04	10.90	31.59	6.69	45.18	298.67	7.90	0.53	0.84
3	171.67	67.95	114.89	138.30	49.43	149.11	38.01	147.87	10.13	34.94	827.80	9.12	0.50	1.20
5	296.85	96.75	214.32	302.70	75.15	193.64	102.84	186.95	55.55	13.81	1394.05	7.62	0.51	1.41
7	147.08	58.64	92.69	100.05	31.43	117.70	30.54	114.63	7.59	25.54	661.33	7.31	0.51	1.08
9	216.41	77.35	128.49	185.77	35.47	140.66	41.10	135.64	10.26	70.27	925.42	5.51	0.51	1.45
13	219.51	68.80	134.48	172.91	27.71	123.05	32.38	113.23	11.08	42.31	864.36	4.44	0.52	1.29
15	184.23	83.91	113.98	131.43	38.04	147.92	39.40	143.53	7.32	21.97	844.40	6.90	0.51	1.15
17	172.77	62.30	104.63	130.11	25.22	106.24	32.99	102.18	7.78	33.29	711.22	5.10	0.51	1.24
27	202.42	81.91	123.07	138.10	43.53	162.26	43.47	154.43	9.06	24.58	905.66	7.39	0.51	1.12
29	276.48	109.38	182.70	244.55	27.32	159.19	37.77	93.39	8.48	14.41	1103.45	3.25	0.63	1.34
31	263.86	83.63	129.97	140.68	43.00	187.08	48.12	163.84	5.90	18.54	1017.17	6.50	0.53	1.08
33	199.84	82.09	124.12	140.72	47.75	173.47	48.96	167.03	7.21	22.76	936.24	8.03	0.51	1.13
35	202.26	81.28	131.53	142.45	41.51	186.10	48.75	185.06	5.67	15.45	977.42	6.93	0.50	1.08
37	259.41	102.11	156.20	173.22	45.26	215.48	61.67	203.83	6.51	22.31	1171.91	6.15	0.51	1.11
39	279.59	108.69	171.83	185.55	48.72	229.13	63.03	218.62	8.90	26.79	1256.43	6.13	0.51	1.08
41	303.85	109.65	173.17	238.66	35.11	182.52	47.89	173.59	10.89	19.28	1229.33	4.08	0.51	1.38
43	310.36	121.24	187.83	193.14	47.48	249.97	71.91	237.13	8.46	28.26	1371.58	5.52	0.51	1.03
45	266.77	115.62	163.79	165.36	44.46	211.07	55.49	197.02	5.88	18.17	1175.12	5.88	0.52	1.01
47	386.19	141.89	223.71	244.24	55.05	301.79	84.46	281.40	12.66	38.69	1663.69	5.24	0.52	1.09
49	368.07	137.32	189.83	361.29	37.39	261.02	76.15	257.90	13.54	29.74	1651.57	3.42	0.50	1.90
53	425.54	164.45	235.02	261.47	55.60	319.93	87.12	294.91	10.93	37.31	1788.43	4.87	0.52	1.11
55	353.11	132.72	186.33	212.34	44.68	253.00	68.28	227.48	9.78	31.05	1433.27	4.81	0.53	1.14
57	371.19	143.91	183.08	219.11	50.58	277.80	78.02	254.34	10.42	40.53	1527.45	5.23	0.52	1.20
59	412.11	149.37	204.71	227.93	48.08	299.46	74.23	274.21	8.47	27.54	1642.03	4.61	0.52	1.11
61	259.87	101.90	125.06	151.81	30.67	188.40	48.09	177.39	5.24	16.28	1052.53	4.58	0.52	1.21
65	160.19	66.67	83.10	95.03	20.70	134.82	30.08	128.23	1.58	3.78	698.13	4.86	0.51	1.14
67	138.41	54.68	70.27	76.81	17.44	113.66	22.63	109.21	1.93	5.32	585.67	4.88	0.51	1.09
69	156.47	60.95	62.32	67.69	19.78	130.88	24.77	132.72	3.37	7.96	635.80	5.39	0.50	1.09
71	133.83	53.98	62.31	64.15	17.08	109.55	21.02	106.20	2.08	12.64	551.04	5.16	0.51	1.03

BbFl: Benzo(b)fluoranthene; BkFl: Benzo(k)fluoranthene; BePy: Benzo(e)Pyrene; BaPy: Benzo(a)Pyrene; Pe: Perylene; IPy: Indeno(1,2,3-cd)pyrene; DBahA: Dibenz(a,h)anthracene; BghiPe: Benzo(ghi)perylene; 2,6DMPh: 2,6-dimethylphenanthrene; 1,7DMPh: 1,7-dimethylphenanthrene; BFl: (Benzo(b)fluoranthene; Benzo(k,j)fluoranthene).

using the Mann-Whitney U test (p < 0.05) the values for the latter period are significantly larger than for the former period. This can be taken as an indication of PAH apportioning from nearer non-atmospheric sources such as runoff from roads and highways constructed or enlarged in recent times in the coastline surrounding the sampling station. A significant fraction of liquid fossil fuel combustion PAH and BC component may enter the bay through this route.
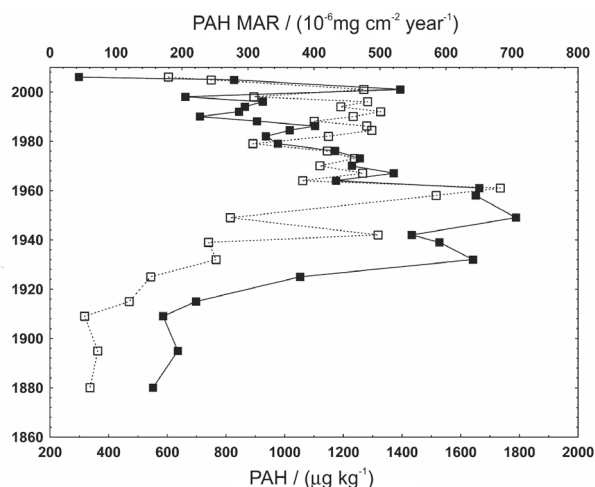
Figure 7. Depth profile of PAH concentration (closed squares) and PAH Mass Accumulation Rates (PAH MAR; open squares).

BaPy increases sharply from 1909 to 1958 reaching a maximum of 361 μg kg^{-1} and then declines to an average of 170 ± 51 μg kg^{-1} (Table 3). It is worthy of note that after 1915 all segments show BaPy concentrations above the Threshold Effect Level (88.8 μg kg^{-1})[48] and therefore they are likely to cause toxicity to exposed organisms.

The only exception in recent times is the sediment from 2006 that shows 50 μg kg^{-1} although reduction in PAH concentration is remarkable since 1960s. In more recent years the decline in BaPy and other combustion related PAH may also be ascribed to changes in the legislation targeting reduction of emissions from light vehicles and enforced in three steps including: in 1988 modernization of motors, in 1992 use of oxidation catalysts, and in 1997 use of three way catalysts (TWC). Likewise, the environmental legislation targeting reduction of industrial emissions made progress, which contributed to lower PAH concentrations after the 1990s. The economic decline following the oil crisis in 1976 endured until the beginning of the 1990s and may be considered an additional factor influencing the observed PAH trends during this period. The consequences of the transition from biomass combustion to fossil fuel combustion as a major PAH source, as discussed above, has to be taken into account.

As expected from the 15% variation in BaPy/BePy ratio found for the entire data set, BaPy is significantly correlated to BePy (y = 15.7 + 1.31x; r = 0.975, p << 0.01). BbFl is also correlated to BkFl (y = 4.53 + 2.59x; r = 0.904, p << 0.01). Such highly significant correlations are strong indication that these compounds derive principally from the same source as suggested by Dickhut *et al.*[49] who found significant correlations between PAH isomer pairs in sediments from Chesapeake Bay. In the present work, all HMW PAH are highly correlated and possibly derive primarily from combustion sources.

A variety of diagnostic ratios have been widely used to estimate the origin of PAH present in environmental samples. Some of those are used to distinguish contributions from different pyrolytic sources, as for instance: IPy/(IPy+BghiPe), 1,7DMPh/(2,6+1,7)DMPh and BFl/ (BFl+BePy).[3,49,50]

The IP/IP+BghiPe (Table 3) of 0.51 ± 0.009 (only a sample from 1986 gave 0.63) exceeds by only 0.01 the upper threshold given for indication of PAH derived from liquid fossil fuel combustion, therefore one can assume there is a component from this source and possibly some contribution from biomass combustion in all samples. There are no trends of the ratio with time and consequently it does not effectively indicate changes in contribution from different combustion sources. Differently, in Figure 8 the cross plot of BFl/(BFl+BePy) and 1,7DMP/(2,6+1,7DMPh) ratios show a number of samples grouped in three sets according to the former ratio: a group with a ratio of < 0.7 in which PAH derives from fuel combustion (segments 1, 3, 5, 7, 13, 17, 29, 33, 35 and 39); a second group on the border line (ratio = 0.7) between fuel and biomass combustion as PAH sources (segments 9, 15, 27, 37, 41, 43, 45 and 47); and a third group with ratios > 0.7 characterizing
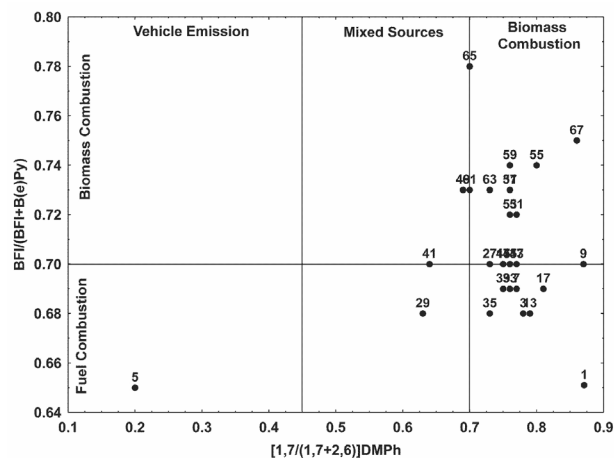
Figure 8. Cross plot of PAH diagnostic ratios. Benzo(b,k,j)fluoranthene (BFl), benzo(e)pyrene (B(e)Py), 1,7-dimethylphenanthrene (1,7DMPh), 2,6-dimethylphenanthrene (2,6DMPh).

biomass combustion as the PAH source. The threshold of 0.7 proposed by Yunker *et. al.*[3] was used here as a sharp boundary; however, some changes due to differential degradation and other factors cannot be ruled out.

The assumption that the threshold of 0.7 holds leads to conclusions coherent with the historical developments. In the first two groups (fossil fuel and borderline) are all samples from the period between 1961 and 2006, except for sample 31 (1984) and in the last group are all samples from before the 1960s. Note also that the difference of the ratio value from 0.7 increases with the age of the sediment layer. Therefore the ratio BFl/(BFl+BePy) seems to produce reliable source diagnosis for PAH emitted from combustion processes to the studied sediments. The 1,7DMP/(1,7+2,6) DMPh ratio, however, was not effective in separating samples. According to this ratio most samples contain PAH from biomass combustion with few in which PAH derive from mixed sources (segments 29, 41, 49, 61, 65) and in segment 5 (sample possibly contaminated by residues of MF380 oil) from fuel combustion.

The difficulty in source assignment using the diagnostic ratios results from differential degradation of the compounds but also from differential settling of particles which is size dependent.[31]

Perylene must be evaluated carefully since it may be formed due to diagenesis of organic matter but can also be generated from incomplete combustion processes. The ratio of perylene to the sum of the pentacyclic PAH (i.e., benzo(b)fluoranthene, benzo(k)fluoranthene, benzo(a) pyrene, benzo(e)pyrene and perylene) when smaller than 10% suggests a pyrolytic origin for the compound.[51] The average value of 5.67% ± 1.39% for the entire core, the lack of a clear Pe concentration trend over time, and the statistically significant correlation of perylene with all the other HMW PAH ($0.65 < r < 0.88$; $p < 0.05$) are robust evidence of a combustion component for this compound.

Conclusions

Although BC is qualitatively a reliable marker of combustion processes the search for quantitative information on changes over time is not trivial. All methods so far available for BC determination have limitations. The combustion method determines soot BC and does not provide information on the major fraction of BC formed during biomass combustion. Being able to quantify this source is of key importance in reconstructing combustion impact in regions where fire is used to clear forested land, harvesting or to prepare the land for new plantations. The SEM is an expensive technique that requires elimination of matrix components using either thermal or chemical oxidation of amorphous organic carbon and chemical elimination of other interfering solids. The NMR is an adequate technique to determine the full spectrum of BC; however it also requires extensive treatment of samples. In both cases, where extensive treatment and sample manipulation is required there are serious risks of losses. In the present high-resolution study of a dated sediment core, the availability of sample is limited and working with smaller masses aggravates the problems of detection. The effectiveness of the NMR determinations was principally affected by the reduced sample mass and the consequently longer measurement times needed. Nevertheless the presence of aromatic carbon associated to BC was detected and varied in the range of 8-16%.

The examined sediments show relatively high TOC content and in the SEM the predominance of diatoms relics is a historical proof of the long lasting anthropogenic fertilization of the bay. The contribution of BC to TOC varied from 6 to 18% and is a significant fraction of the organic carbon pool. A decrease in this contribution is evident in the last 30 years due to increasing eutrophication of the system coupled to reduction of BC emissions due to the ethanol use and modernization of the automotive fleet.

The multiple approaches so far used to evaluate the origin of combustion residues and the change with time of inputs to the Guanabara Bay provided data, which can be understood on the basis of the historical developments in the region. The main factors influencing quantitative PAH and BC records in the sediment were the change with time of predominance of biomass combustion to fossil fuel combustion, the economic decline during the oil crises in the 1970s and the introduction of ethanol in the energy matrix. Qualitatively, the BFl/(BFl+BePy) was the most effective ratio in characterizing the change over time of the combustion sources.

Acknowledgments

Supplementary Information

Supplementary Information (Figure S1) is available free of charge at http://jbcs.sbq.org.br, as PDF file.

References

1. Highwood, E. J.; Kinnersley, R. P.; *Environ. Int.* **2006**, *32*, 560.

2. Koelmans, A. A.; Jonker, M. T. O.; Cornelissen, G.; Bucheli, T. D.; Noort, P. C. M. V.; Gustafsson, Ö.; *Chemosphere* **2006**, *63*, 365.

3. Yunker, M. B.; Macdonald, R. W.; Vingarzan, R.; Mitchell, R. H.; Goyette, D.; Sylvestre, S.; *Org. Geochem.* **2002**, *33*, 489.

4. Buckley, D. R.; Rockne, K. J.; Li, A.; Mills, W. J.; *Environ. Sci. Technol.* **2004**, *38*, 1732.

5. Mannino, A.; Harvey, H. R.; *Limnol. Oceanogr.* **2004**, *49*, 735.

6. Grossman, A.; Ghosh, U.; *Chemosphere* **2009**, *75*, 469; Zhang, Y.; Schauer, J. J.; Zhang, Y.; Zeng, L.; Wei, Y.; Liu, Y.; Shao, M.; *Environ. Sci. Technol.* **2008**, *42*, 5068.

7. Gustafsson, Ö.; Gschwend, P. M.; *Geochim. Cosmochim. Acta* **1998**, *62*, 465.

8. Gustafsson, Ö.; Haghseta, A.; Chan, C.; MacFarlane, J.; Gschwend, P. M.; *Environ. Sci. Technol.* **1997**, *31*, 203.

9. Jonker, M. T. O.; Koelmans, A. A.; *Environ. Sci. Technol.* **2002**, *36*, 3725; Lohmann, R.; MacFarlane, J. K.; Gschwend, P. M.; *Environ. Sci. Technol.* **2005**, *39*, 141; Oen, A. M.; Cornelissen, G.; Breedveld, G. D.; *Environ. Pollut.* **2006**, *141*, 370.

10. Ribeiro, L. G. L.; Carreira, R. S.; Wagener, A. L. R.; *J. Braz. Chem. Soc.* **2008**, *19*, 1277.

11. Hung, C. C.; Gong, G. C.; Ko, F. C.; Chen, H. Y.; Hsu, M. L.; Wu, J. M.; Peng, S. C.; Nan, F. H.; Yeager, K. M.; Santschi, P. H.; *Mar. Pollut. Bull.* **2010**, *60*, 1010.

12. Cornelissen, G.; Gustafsson, Ö.; *Environ. Sci. Technol.* **2004**, *38*, 148.

13. Ver, L. M. B.; Mackenzie, F. T.; Lerman, A.; *Chem. Geol.* **1999**, *159*, 283.

14. Farias, C. O.; Hamacher, C.; Wagener, A. L. R.; Scofield, A. L.; *Org. Geochem.* **2008**, *39*, 289.

15. Instituto Estadual do Ambiente (INEA); *Relatório Anual da Qualidade do Ar do Estado do Rio de Janeiro (2009)*; available at http://www.inea.rj.gov.br/downloads/relatorios/qualidade_ar_2009.pdf accessed in August, 2013.

16. Godoy, J. M.; Oliveira, A. V.; Almeida, A. C.; Godoy, M. L. D. P.; Moreira, I.; Wagener, A. R.; Figueiredo Jr., A. G. D.; *J. Braz. Chem. Soc.* **2012**, *23*, 1265.

17. Borges, A. C.; Sanders, C. J.; Santos, H. L.; Araripe, D. R.; Machado, W.; Patchineelam, S. R.; *Mar. Pollut. Bull.* **2009**, *58*, 1750.

18. Secretaria Municipal de Transporte (SMTR); available at http://obras.rio.rj.gov.br/index2.cfm?sqncl_publicacao=250 accessed in August, 2013.

19. Rocha Filho, P.; *Relatório final de avaliação das condições presentes de funcionamento do complexo industrial REDUC/DTSE sob o ponto de vista de suas implicações ambientais*. RIO DE JANEIRO Secretaria de Estado de Ciência e Tecnologia. Rio de Janeiro: A Secretaria, 2000.

20. Carreira, R. S.; Wagener, A. L. R.; Readman, J. W.; Fileman, T. W.; Macko, S. A.; Veiga, A.; *Mar. Chem.* **2002**, *79*, 207.

21. Hammes, K.; Schmidt, M. W. I.; Smernik, R. J.; Currie, L. A.; Ball, W. P.; Nguyen, T. H.; Louchouarn, P.; Houel, S.; Gustafsson, Ö.; Elmquist, M.; Cornelissen, G.; Skjemstad, J. O.; Masiello, C. A.; Song, J.; Peng, P. A.; Mitra, S.; Dunn, J. C.; Hatcher, P. G.; Hockaday, W. C.; Smith, D. M.; Hartkopf-Fröder, C.; Böhmer, A.; Lüer, B.; Huebert, B. J.; Amelung, W.; Brodowski, S.; Huang, L.; Zhang, W.; Gschwend, P. M.; Flores-Cervantes, D. X.; Largeau, C.; Rouzaud, J.-N.; Rumpel, C.; Guggenberger, G.; Kaiser, K.; Rodionov, A.; Gonzalez-Vila, F. J.; Gonzalez-Perez, J. A.; de la Rosa, J. M.; Manning, D. A. C.; López-Capél, E.; Ding, L.; *Global Biogeochem. Cy.* **2007**, *21*, GB3016.

22. Louchouarn, P.; Chillrud, S. N.; Houel, S.; Yan, B.; Chaky, D.; Rumpel, C.; Largeau, C.; Bardoux, G.; Walsh, D.; Bopp, R. F.; *Environ. Sci. Technol.* **2007**, *41*, 82.

23. Gustafsson, Ö.; Bucheli, T. D.; Kukulska, Z.; Andersson, M.; Largeau, C.; Rouzaud, J.-N.; Reddy, C. M.; Eglinton, T. I.; *Global Biogeochem. Cy.* **2001**, *15*, 881.

24. Gélinas, Y.; Baldock, J. A.; Hedges, J. I.; *Org. Geochem.* **2001**, *32*, 677.

25. De La Rosa, J. M.; González-Pérez, J. A.; Hatcher, P. G.; Knicker, H.; González-Vila, F. J.; *Eur. J. Soil Sci.* **2008**, *59*, 430.

26. Simpson, M.; Hatcher, P. G.; *Org. Geochem.* **2004**, *35*, 923.

27. PLANÁGUA/SEMADS/GTZ; *Cooperação Técnica Brasil/Alemanha*; SEMADS: Rio de Janeiro, 2001.

28. Wagener, A. L. R.; *Quím. Nova* **1995**, *18*, 534.

29. Meyers, P. A.; *Chem. Geol.* **1994**, *114*, 289.

30. Associação Nacional dos Fabricantes de Veículos Automotores (ANFAVEA); available at http://www.anfavea.com.br/anuario.html accessed in August, 2013.

31. Masiello, C.; *Mar. Chem.* **2004**, *92*, 201.

32. Catanzaro, L. F.; Baptista Neto, J. A.; Guimarães, M. S. D.; Silva, C. G.; *Rev. Bras. Geof.* **2004**, *22*, 69.

33. Lee, H.; Myung, C.-L.; Park, S.; *Fuel* **2009**, *88*, 1680; Lemaire, R.; Therssen, E.; Desgroux, P.; *Fuel* **2010**, *89*, 3952.

34. Luz, L. G.; Carreira, R. S.; Farias, C. O.; Scofield, A. D. L.; Nudi, A. H.; Wagener, A. D. L. R.; *Org. Geochem.* **2010**, *41*, 1146.

35. Accardi-Dey, A.; Gschwend, P. M.; *Environ. Sci. Technol.* **2003**, *37*, 99.

36. Rockne, K. J.; Shor, L. M.; Young, L. Y.; Taghon, G. L.; Kosson, D. S.; *Environ. Sci. Technol.* **2002**, *36*, 2636.

37. Stoffyn-Egli, P.; Potter, T. M.; Leonard, J. D.; Pocklington, R.; *Sci. Total Environ.* **1997**, *198*, 211.

38. Brodowski, S.; Amelung, W.; Haumaier, L.; Abetz, C.; Zech, W.; *Geoderma* **2005**, *128*, 116.

39. Glaser, B.; Balashov, E.; Haumaier, L.; Guggenberger, G.; Zech, W.; *Org. Geochem.* **2000**, *31*, 669.

40. Song, J.; Peng, P. A.; Huang, W.; *Environ. Sci. Technol.* **2002**, *36*, 3960.

41. Godoi, R. H. M.; Godoi, A. F. L.; Worobiec, A.; Andrade, S. J.; de Hoog, J.; Santiago-Silva, M. R.; Grieken, R. V.; *Microchim. Acta* **2004**, *145*, 53.

42. Tumolva, L.; Park, J.-Y.; Kim, J.-S.; Miller, A. L.; Chow, J. C.; Watson, J. G.; Park, K.; *Aerosol Sci. and Technol.* **2010**, *44*, 202.

43. Dai, K. O. H.; Johnson, C. E.; *Geoderma* **1999**, *93*, 289.

44. Rumpel, C.; Chaplot, V.; Chabbi, A.; Largeau, C.; Valentin, C.; *Geoderma* **2008**, *145*, 347; Lorenz, K.; Preston, C.; Kandeler, E.; *Geoderma* **2006**, *130*, 312.

45. Lu, X. Q.; Hanna, J. V.; Johnson, W. D.; *Appl. Geochem.* **2000**, *15*, 1019.

46. Mengchang, H.; Yehong, S.; Chunye, L.; *J. Environ. Sci.* **2008**, *20*, 1294.

47. Flores-Cervantes, D. X.; Plata, D. L.; MacFarlane, J. K.; Reddy, C. M.; Gschwend, P. M.; *Mar. Chem.* **2009**, *113*, 172.

48. Buchman, M. F.; *NOAA screening quick reference tables,* NOAA OR&R Reports 08-1; Office of Response and Restoration Division, National Oceanic and Atmospheric Administration: Seattle, WA, 2008.

49. Dickhut, R. M.; Canuel, E. A.; Gustafson, K. E.; Liu, K.; Arzayus, K. M.; Walker, S. E.; Edgecombe, G.; Gaylor, M. O.; MacDonald, E. H.; *Environ. Sci. Technol.* **2000**, *34*, 4635.

50. Katsoyiannis, A.; Terzi, E.; Cai, Q.-Y.; *Chemosphere* **2007**, *69*, 1337.

51. Readman, J. W.; Fillmann, G.; Tolosa, I.; Bartocci, J.; Villeneuve, J.-P.; Catinni, C.; Mee, L. D.; *Mar. Pollut. Bull.* **2002**, *44*, 48; Jiang, J. J.; Lee, C. L.; Fang, M. D.; Liu, J. T.; *Mar. Pollut. Bull.* **2009**, *58*, 752.

Supplementary Information

Reconstructing Historical Changes in Combustion Patterns by Means of Black Carbon and PAH Evaluation in Dated Sediments from Guanabara Bay, Rio de Janeiro

Cristiane R. Mauad,[a] Angela de L. R. Wagener,*,#,[a] Cássia de O. Farias,[a]
Naira M. S. Ruiz,[b] Renato S. Carreira,[a] Crisógono Vasconcelos,[c] José M. Godoy,[a]
Sonia M. C. de Menezes,[b] Arthur de L. Scofield[a]

[a]*LABMAM, Departamento de Química, Pontifícia Universidade Católica do Rio de Janeiro,*
20453-900 Rio de Janeiro-RJ, Brazil.

[b]*CENPES-PETROBRAS, Avenida Horácio Macedo, 950, Cidade Universitária,*
Ilha do Fundão, 21941-915 Rio de Janeiro-RJ, Brazil.

[c]*Laboratory of Geomicrobiology, ETH/Zürich, Sonneggstrasse 5, 8092 Zürich, Switzerland.*

Figure S1. SEM of centric diatoms found in the segment 39.

*e-mail: angela@puc-rio.br
#present address: Faculdade de Oceanografia, Universidade do Estado do
Rio de Janeiro, 20550-013 Rio de Janeiro-RJ, Brazil